High efficiency KTiOAsO$_4$ optical parametric oscillator within a diode-side-pumped two-rod Nd:YAG laser

W.J. Sun · Q.P. Wang · Z.J. Liu · X.Y. Zhang · F. Bai · X.B. Wan · G.F. Jin · X.T. Tao · Y.X. Sun

Abstract A high efficiency KTiOAsO$_4$(KTA) intracavity optical parametric oscillator (IOPO) is demonstrated within a diode-side-pumped acousto-optically (AO) Q-switched two-rod Nd:YAG laser. With a 25-mm-long X-cut KTA crystal, efficient parametric conversions to signal (1.54 μm) and idler (3.47 μm) waves are realized. The highest output power of 15.8 W including 12.7 W signal and 3.1 W idler power is obtained at a repetition rate of 7.5 kHz and a pump power of 208 W, corresponding to an optical-to-optical conversion efficiency of up to 7.6%. The signal pulse duration is 32 ns with a peak power of 53 kW. At a repetition rate of 12.5 kHz and the pump power of 208 W, the highest idler power of 3.4 W is obtained with a peak power of 14 kW and a pulse duration of 19 ns. And the beam quality factors (M^2) of the signal and idler waves are determined to be around 2 and 20, respectively.

1 Introduction

The need for powerful tunable laser sources has brought about important development of optical parametric oscilla-

W.J. Sun · Q.P. Wang · Z.J. Liu (✉) · X.Y. Zhang · F. Bai ·
X.B. Wan · G.F. Jin
School of Information Science & Engineering, Shandong
University, Jinan, Shandong 250100, P.R. China
e-mail: zhaojunliu@sdu.edu.cn
Fax: +86-531-88362358

W.J. Sun · Q.P. Wang · Z.J. Liu · X.Y. Zhang · F. Bai · X.B. Wan
Shandong Provincial Key Laboratory of Laser Technology and
Application, Shandong University, Jinan, Shandong 250100,
P.R. China

X.T. Tao · Y.X. Sun
Institute of Crystal Materials, Shandong University, Jinan,
Shandong 250100, P.R. China

tors (OPOs) in recent years [1–5]. OPOs are inherently high-efficiency solid-state light sources, which can provide wavelength tunability unobtainable with conventional solid-state laser. OPOs are usually applied to realize the eye-safe wavelength region [6–8], 2 μm region [9, 10] and mid-infrared (mid-IR) region [11–13]. Many nonlinear crystals are chosen in OPOs to generate different wavelengths. One kind of the nonlinear crystals are those periodically poled crystals, such as PPLN (Periodically Poled LiNbO$_3$), PPKTP (Periodically Poled KTiOPO$_4$), PPRTA (Periodically Poled RbTiOAsO$_4$), etc. [12–15]. Recently, Peng et al. reported the high-efficiency mid-IR OPO based on PPMgO:CLN [13]. And Pelitz et al. reported 2 W and 1.3 W total output power OPOs based on PPKTP and PPRTA, respectively [14]. Another kind of crystals, such as ZnGeP$_2$ (ZGP), AgGaS$_2$, LiInSe$_2$, and CdSiP$_2$ [16–19], are also employed to realize mid-IR OPOs. For example, Dergachev achieved a near diffraction-limited beam at 3.4 μm with pulse energy of 10 mJ with a ZGP nanosecond OPO [16]. Petrov et al. reported a subnanosecond, 1 kHz, temperature-tuned, noncritical mid-IR OPO based on CdSiP$_2$ crystal [19]. KTiOPO$_4$ (KTP) and its isomorphs have also been widely used in OPOs for many advantages [7, 8, 20–22]. And the property of noncritical phase matching (NCPM) is the most important one. This indicates a large acceptance angle for efficient parametric conversions even with multitransverse-mode pumping lasers. Compared with KTP, KTiOAsO$_4$ (KTA) has higher transmission in the 3–5 μm region and does not have the absorption feature seen in KTP near 3.47 μm [23]. This makes KTA more attractive than KTP in high power mid-IR OPOs. Wu et al. achieved 4.1 W at 3.5-μm output and 15 W total output from a KTA OPO pumped by Nd:YALO laser, and the total efficiency was 2.6% [11]. Zhong et al. achieved 31 mJ output energy at 3.47 μm from a side-pumped electrooptical (EO) Q-switched Nd:YAG laser

based on KTA OPO; its absolute optical-to-optical conversion efficiency was 4.76% [20]. Our group has made some research in eye-safe KTA OPOs. We reported high efficiency AO Q-switched intracavity Nd:YAG/KTA OPO at 1535 nm with the optical-optical conversion efficiency of up to 12.5% [4]. And we also reported the 2.54 W 1535 nm KTA OPO within a side-pumped AO Q-switched Nd:YAG laser in 2008 [8].

In this paper, we demonstrate a high power, high efficiency, intracavity KTiOAsO$_4$ optical parametric oscillator. The pump source is a diode-side-pumped two-rod Nd:YAG laser. A 90° quartz rotator is inserted between the two Nd:YAG modules to compensate the birefringence. An AO Q-switch is used to obtain nanosecond pulses. A 25-mm-long X-cut KTA crystal is used in the experiment. The highest average output power of 12.7 W at 1.54 μm and 3.1 W at 3.47 μm are obtained at the pulse repetition rate (PRR) of 7.5 kHz under the diode power of 208 W, corresponding to an optical-to-optical conversion efficiency of up to 7.6%. This is the highest conversion efficiency in diode-side-pumped KTA IOPOs to our knowledge. The pulse width of the signal wave is measured to be 32 ns corresponding to a peak power of 53 kW. At a repetition rate of 12.5 kHz and pump power of 208 W, we obtain the highest idler power of 3.4 W. The idler peak power is 14 kW with a pulse duration of 19 ns. The beam quality factors (M^2) of the 3.47 μm wave are measured to be 21.2 ± 0.2 and 20.2 ± 0.2 in the horizontal and vertical directions, respectively. And those for the signal wave are 2.1 ± 0.2 and 2.2 ± 0.2, respectively.

2 Experimental setup

The experimental configuration of the KTA OPO is shown in Fig. 1. The rear mirror (RM) was an 800 mm radius-of-curvature convex mirror and was coated for high-reflection (HR) at 1064 nm ($R > 99.8\%$). The convex-plane cavity was used to keep a relative large laser mode size under high pump power. The 40-mm-long AO Q-switch had antireflection (AR) coatings at 1064 nm ($R < 0.2\%$) on both faces. It was driven at 27.12 MHz center frequency with the radiofrequency power of 50 W. Two same laser heads were employed in the experiments. Each one consisted of an Nd:YAG rod (0.6 at. %, $\varnothing 3$ mm $\times$ 63 mm), a cooling

sleeve, a diffusive optical pump cavity, and three diode array modules. The 90° quartz rotator was AR coated on both faces at 1064 nm ($R < 0.5\%$). M_1 was made of infrared optical quartz glass. Its coatings were AR at 1.06 μm ($R < 0.2\%$) and HR ($R > 99.5\%$) at both the signal wavelength (1.54 μm) and the idler wavelength (3.47 μm). The output coupler (OC) was made of CaF$_2$ to avoid mid-IR absorption. It was coated for HR at 1064 nm, partial-reflection at the signal wavelength ($R = 80\%$) and high-transmission (HT) at the idler wavelength ($T > 95\%$). Hence, this KTA OPO was a singly resonated OPO (SRO). A type II non-critical phase-matching KTA crystal (X-cut, $\theta = 90°$, $\phi = 0°$) with a size of $4 \times 4 \times 25$ mm^3 was employed in our experiment. Both faces of the KTA crystal were AR coated at both 1.54 μm and 1.06 μm ($R < 0.2\%$) and the coatings were HT at 3.47 μm ($T > 97\%$). The Nd:YAG laser modules and the Q-switch were water cooled with the water temperature of 20°C. The KTA crystal was wrapped with indium foil and mounted in water-cooled copper blocks. The water temperature was also maintained at 20°C. The rear mirror, the AO Q-switch, the quartz rotator and the Nd:YAG rods were all positioned close to each other. The cavity lengths of the whole and OPO cavities were 515 mm and 185 mm, respectively. The KTA crystal was placed in the middle of the OPO cavity.

3 Results and discussions

The wavelengths of the fundamental and signal waves were measured by a wide-range optical spectrum analyzer with a spectra range from 350 to 1750 nm. The idler spectrum was monitored with an infrared spectral analyzer. The optical spectra of the signal and idler waves are shown in Fig. 2(a) and Fig. 2(b), respectively. From Fig. 2, the signal wavelength was determined to be 1535 nm and the idler wavelength was determined to be 3467 ± 3 nm.

A dichroic mirror (DM$_1$, CaF$_2$ material) coated for HT ($T > 99\%$) at 3.47 μm and HR ($R > 99.5\%$) at both 1.54 μm and 1.06 μm was used to separate the fundamental, signal and idler waves. Another mirror (DM$_2$, BK7 glass) was also used to separate the fundamental wave and signal wave or to attenuate the power. When we measured the powers, DM$_2$ was chosen to be such a mirror that coated for HR at 1.06 nm ($R > 99.5\%$) and HT at 1.54 nm ($T > 99.5\%$).

Fig. 1 Schematic diagram of the intracavity KTA OPO: *RM*—rear mirror; *AO*—acousto-optical Q-switch; *KTA*—X-cut KTiOAsO$_4$ crystal; *OC*—output coupler

RM AO Quartz rotator M$_1$ OC DM$_1$

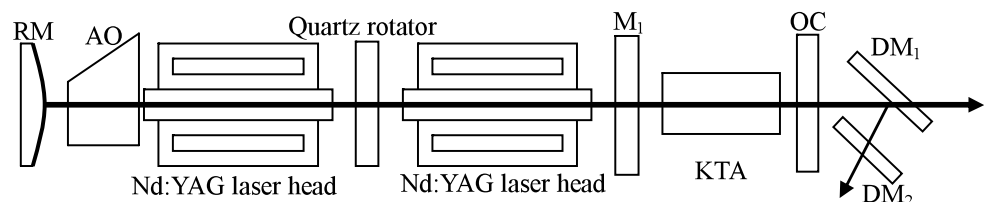Nd:YAG laser head   Nd:YAG laser head   KTA   DM$_2$

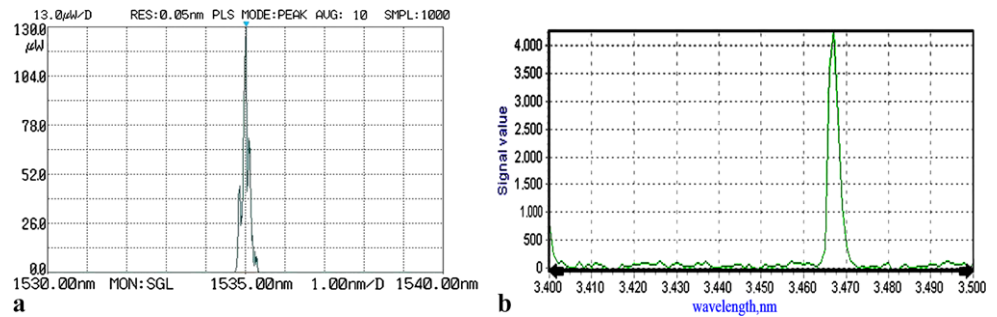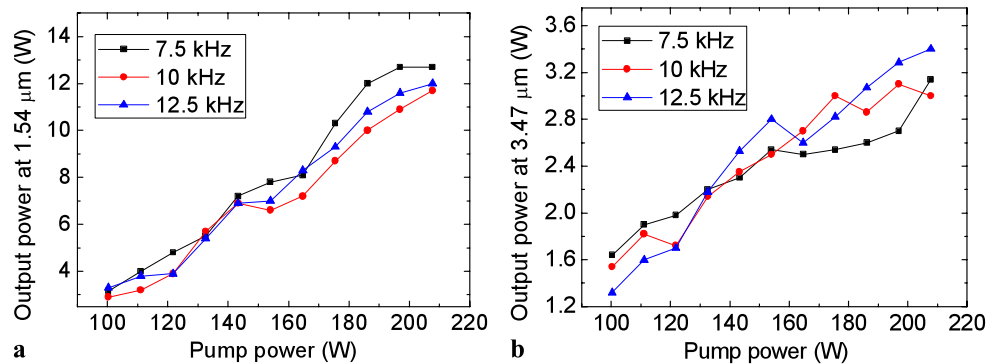**Fig. 2** Optical spectra of signal and idler waves: (**a**) signal; (**b**) idler

Fig. 3 Output power versus input diode power at different PRRs: (**a**) signal; (**b**) idler

We measured the output power by an EPM 2000 power meter. Output powers at 1.54 μm and 3.47 μm versus input pumping power at different repetition rates are shown in Fig. 3(a) and Fig. 3(b), respectively.

The highest signal power of 12.7 W was obtained at a pump power of 208 W and a PRR of 7.5 kHz. Under this condition, the total power was 15.8 W, corresponding to an optical-optical conversion efficiency of 7.6%. This is the highest conversion efficiency in diode-side-pumped KTA IOPO to our knowledge. With a diode power of 208 W and a repetition rate of 12.5 kHz, the highest idler power of 3.4 W was obtained. Simultaneously, we obtained the signal power of 12 W.

We attribute the high conversion efficiency and high output power to the cavity design. Firstly, the fundamental wave cavity was designed for stable operation with large mode volume at high pump power. The convex rear mirror could increase the mode size of the fundamental wave, therefore, the diffraction loss of high-order transverse modes of the fundamental wave increased, which led to better beam quality of the fundamental wave. As depicted in [24], the lower-order laser transverse modes generate the OPO output more efficiently than the higher-order ones. As a result, the OPO conversion efficiency increased. And the 90° quartz rotator was inserted between two Nd:YAG rods to compensate thermal induced birefringence, which would expand the cavity stable region for the fundamental wave. Secondly, the OPO cavity was designed considering the mode match. Total output powers versus input diode power for OPO cavity lengths
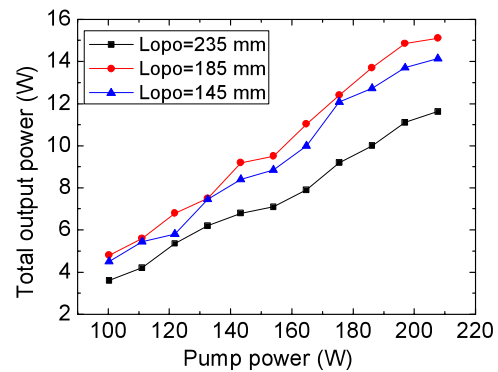

Fig. 4 Total output powers versus input diode power for OPO cavity lengths of 145, 185, and 225 mm

of 145, 185, and 225 mm are shown in Fig. 4. The longer OPO cavity length could increase the signal mode volume, which led to good mode match, and hence high conversion efficiency and high output power. But under the condition of a stable oscillation cavity, with the OPO cavity length increasing, the overlap of the pump wave and signal wave could decrease. So, the optimum OPO cavity length of about 185 mm was selected.

The temporal characteristics of the signal and mid-IR idlers waves were monitored by a digital phosphor oscilloscope and detected by a fast HgGdZnTe photoconductive detector. The powers totally reflected by DM₁ were very high. In order to avoid damaging the detector, the power must be attenuated. Then another mirror DM₂ coated for HR at

Fig. 5 Temporal pulse shapes of signal and idler waves: (**a**) signal; (**b**) idler
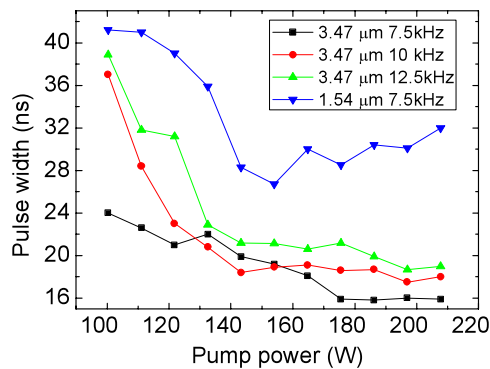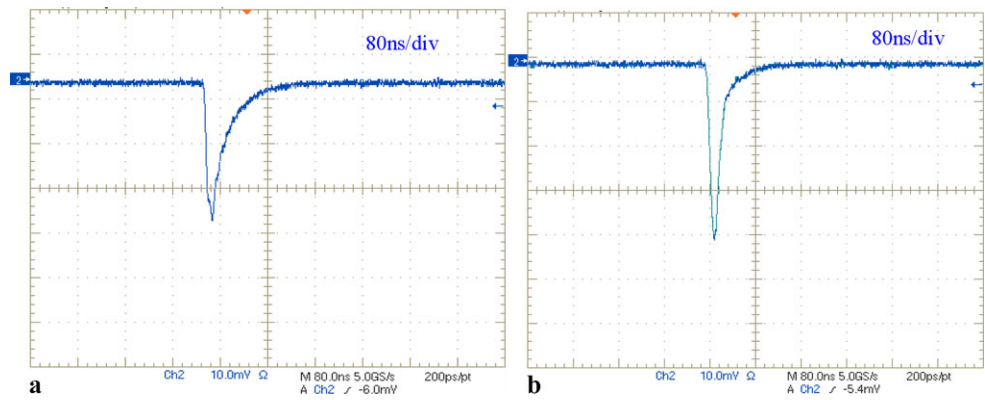

Fig. 6 Pulse widths versus input diode power at different PRRs

1064 nm ($R > 99.5\%$) and partial-reflection ($R = 80\%$) at 1535 nm was chosen. The typical pulse shapes are shown in Fig. 5, where (a) and (b) displays the pulse shape of signal and idler waves, respectively. And Fig. 5 corresponded to the case with pump power of 208 W and PRR of 12.5 kHz.

Pulse widths of the idler wave at the PRRs of 7.5, 10 and 12.5 kHz are shown in Fig. 6. And pulse widths of the signal wave at 7.5 kHz are given for comparison. Each point in Fig. 6 was obtained by averaging arbitrary 10 pulse-width values recorded from the digital oscilloscope. It is evident that at the same pump power and same PRR, the idler pulse duration was much shorter than the signal one. In singly resonated OPO, the idler wave does not oscillate, which means that the cavity loss of the idler wave is much larger than that of the signal wave. Larger cavity loss results in short photon lifetime and hence short pulse duration. Therefore, qualitative analysis indicates that the idler pulse duration is shorter than the signal pulse duration. Quantitative analysis of this phenomenon will be done in the future.

The pulse widths of either signal or idler wave decreased with the pump power increasing. And the pulse widths increased with the repetition rates increasing. Taking the case at a diode power of 208 W as an example, the pulse widths of the idler wave increased from 16 ns to 19 ns with PRRs from 7.5 kHz to 12.5 kHz. At the highest output idler power of 3.4 W, the idler pulse width was obtained to be 19 ns.

Hence, the idler peak power was calculated to be 14 kW with a pulse energy of 272 µJ. And at the highest output signal power of 12.7 W, a pulse duration of 32 ns was obtained. The signal pulse energy reached 1.69 mJ and peak power was 53 kW.

The beam quality of the signal and idler waves were studied with a NanoScan beam analyzer. The typical beam profiles of the idler wave are shown in Fig. 7, where (a) and (b) shows the three-dimensional and two-dimensional distributions, respectively. By focusing the beam with a ZnSe lens ($f = 100$ mm), we measured the beam quality factors (M^2) of the 3.47 µm idler laser at the highest output power of 3.4 W. The M^2 factors in the horizontal and vertical directions were determined to be 21.2 ± 0.2 and 20.2 ± 0.2, respectively. With the same method, the beam quality factors of the signal wave were determined to be 2.1 ± 0.2 and 2.2 ± 0.2, respectively. The good beam quality of the signal wave resulted from the long OPO cavity, which restricted the generations of higher order modes. And the idler wave did not oscillate in our singly resonated OPO, so the beam quality of the idler wave was worse than that of the signal wave. In order to pursue good mid-IR beam quality, we are designing an idler-resonated KTA OPO.

4 Conclusions

In conclusion, a high-power, high conversion efficiency 1.54 µm and 3.47 µm KTA IOPO pumped by an AO Q-switched two-rod Nd:YAG laser has been demonstrated. Under the pump power of 208 W at 808 nm, a maximum average output power of 12.7 W at signal wavelength of 1.54 µm and 3.1 W at idler wavelength of 3.47 µm were obtained at the repetition rate of 7.5 kHz, corresponding to an optical-to-optical conversion efficiency of up to 7.6%. At a repetition rate of 12.5 kHz and pump power of 208 W, we obtain the highest idler power of 3.4 W and the pulse duration of 19 ns, corresponding to the peak power of 14 kW. The M^2 factors of the 3.47 µm and the 1.54 µm were about 20 and 2, respectively.

Fig. 7 Typical mid-IR beam profiles: (**a**) three dimensions; (**b**) two dimensions
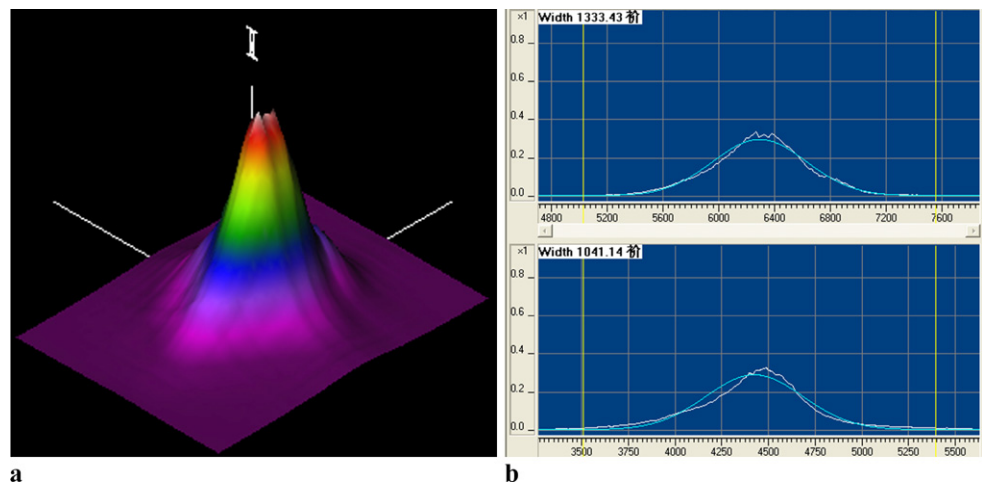
References

1. W.R. Bosenberg, A. Drobshoff, J.I. Alexander, L.E. Myers, R.L. Byer, Opt. Lett. **21**, 1336 (1996)
2. Q. Fu, G. Mak, H.M. van Driel, Opt. Lett. **17**, 1006 (1992)
3. M.S. Webb, P.F. Moulton, J.J. Kasinski, R.L. Burnham, G. Loiacono, R. Stolzenberger, Opt. Lett. **23**, 1161 (1998)
4. Z.J. Liu, Q.P. Wang, X.Y. Zhang, Z.J. Liu, H. Wang, J. Chang, S.Z. Fan, F.S. Ma, G.F. Jin, Appl. Phys. B **90**, 439 (2008)
5. Y. Yashkir, H.M. van Driel, Appl. Opt. **38**, 2554 (1999)
6. W. Żendzian, J.K. Jabczynski, P. Wachulak, J. Kwiatkowski, Appl. Phys. B **80**, 329 (2005)
7. Y.F. Chen, K.W. Su, Y.T. Chang, W.C. Yen, Appl. Opt. **46**, 3597 (2007)
8. Z.J. Liu, Q.P. Wang, X.Y. Zhang, Z.J. Liu, J. Chang, H. Wang, S.Z. Fan, S.T. Li, S.S. Huang, W.J. Sun, G.F. Jin, X.T. Tao, S.J. Zhang, H.J. Zhang, J. Phys. D, Appl. Phys. **41**, 135112 (2008)
9. R.F. Wu, P.B. Phua, K.S. Lai, Y.L. Lim, E. Lau, A. Chng, C. Bonnin, D. Lupinski, Opt. Lett. **25**, 1460 (2000)
10. X.D. Mu, H. Meissner, H.C. Lee, Opt. Lett. **35**, 387 (2010)
11. R.F. Wu, K.S. Lai, H. Wong, W.J. Xie, Y. Lim, E. Lau, Opt. Express **8**, 694 (2001)
12. M.M.J.W. van Herpen, S.E. Bisson, F.J.M. Harren, Opt. Lett. **28**, 2497 (2003)
13. Y.F. Peng, W.M. Wang, X.B. Wei, D.M. Li, Opt. Lett. **34**, 2897 (2009)
14. M. Pelitz, U. Bäder, A. Borsutzky, R. Wallenstein, J. Hellström, H. Karlsson, V. Pasiskevicius, F. Laurell, Appl. Phys. B **73**, 663 (2001)
15. M.A. Arbore, M.M. Fejer, Opt. Lett. **22**, 151 (1997)
16. A. Dergachev, D. Armstrong, A. Smith, T. Drake, M. Dubois, Opt. Express **15**, 14404 (2007)
17. A. Douillet, J.J. Zondy, A. Yelisseyev, S. Lobanov, L. Isaenko, J. Opt. Soc. Am. B **16**, 1481 (1999)
18. J.J. Zondy, V. Vedenyapin, A. Yelisseyev, S. Lobanov, L. Isaenko, V. Petrov, Opt. Lett. **30**, 2460 (2005)
19. V. Petrov, G. Marchev, P.G. Schunemann, A. Tyazhev, K.T. Zawilski, T.M. Pollak, Opt. Lett. **35**, 1230 (2010)
20. K. Zhong, J.Q. Yao, D.G. Xu, J.L. Wang, J.S. Li, P. Wang, Appl. Phys. B **100**, 749 (2010)
21. G.A. Rines, D.M. Rines, P.F. Moulton, in *Advanced Solid State Lasers*, ed. by T. Fan, B. Chai. OSA Proceedings Series, vol. 20 (Optical Society of America, Washington, 1994). Paper PO9
22. H.Y. Zhu, G. Zhang, H.B. Chen, C.H. Huang, Y. Wei, Y.M. Duan, Y.D. Huang, H.Y. Wang, G. Qiu, Opt. Express **17**, 20669 (2009)
23. G.M. Loiacono, D.N. Loiacono, J.J. Zola, R.A. Stolzenberger, T.M. Gee, R.G. Norwood, Appl. Phys. Lett. **61**, 895 (1992)
24. R.F. Wu, P.B. Phua, K.S. Lai, Y.L. Lim, E. Lau, A. Chng, C. Bonnin, D. Lupinski, Opt. Lett. **25**, 1460 (2000)